TECHNICAL MEMORANDUMS

NATIONAL ADVISORY COMMITTEE FOR AERONAUTICS

No. 612

STATIC LONGITUDINAL STABILITY OF "ENTE" AIRPLANES

By Heinrich Georg Kiel

From Zeitschrift für Flugtechnik und Motorluftschiffahrt
December 15, 1930

Washington
March, 1931

NATIONAL ADVISORY COMMITTEE FOR AERONAUTICS

TECHNICAL MEMORANDUM NO. 612

STATIC LONGITUDINAL STABILITY OF "ENTE" AIRPLANES*

By Heinrich Georg Kiel

I. Introduction

The nose-steered or tail-first airplane, the so-called "Ente" (duck), has many advantages over the present normal airplane. Due to the additional lift of the horizontal empennage, the total lift is greater than that of a normal airplane having the same combined area of the wing and horizontal tail surfaces. Moreover, with a correctly dimensioned horizontal empennage, the Ente is stallproof in steady flight, which greatly increases its safety. In considering the static stability, however, we encounter some difficulties which do not appear on an ordinary airplane.

The stability conditions of Ente airplanes are investigated in the present report.** In developing the formulas, which afford an approximate solution, the unimportant effect of the height of the C.G. and the moment of the residual resistance are neglected. Moreover, $c_n = c_a$ is put for both wing and empennage. The effect of the downwash from the forward horizontal empennage on the wing is also disregarded.

*"Die statische Langstabilität der Entenbauart." From Zeitschrift für Flugtechnik und Motorluftschiffahrt, December 15, 1930, pp. 601-610.

**This report was originally written as a student's essay at the Berlin Technical High School with the encouragement of Dr. Martin Schrenk, who also assisted in its elaboration by suggestions and supplementations.

II. Notation

F, wing area (m^2),

b, span (m),

$\Lambda = b^2/F$, aspect ratio of wing,

$t = F/b$, mean wing chord (m),

r, horizontal distance of airplane C.G. from leading edge of wing (+ forward of, and − aft of leading edge) (m),

h, perpendicular distance of the C.G. from the wing chord (disregarded in the investigation) (m),

M, wing moment with respect to leading edge of wing (mkg),

M_F, wing moment with respect to C.G. of airplane (mkg),

α angle of attack of wing,

α_0, " " " " " for $c_a = 0$,

α_{max}, " " " " " " $c_{a\ max}$.

$\alpha_{th} = \alpha - \alpha_0$, theoretical angle of attack of wing with respect to line of zero lift,

$\alpha_{m\ F_0}$, angle of attack of wing at which $c_{m\,F} = 0$,

c_a, lift coefficient of wing,

c_m, moment coefficient of wing with respect to its leading edge,

c_{m_0}, moment coefficient of wing with respect to its leading edge at $c_a = 0$,

c_{mF}, moment coefficient of wing with respect to C.G. of airplane,

c_n, normal force coefficient of wing,

c_t, tangential force coefficient of wing,

l_H, distance of C.G. of airplane from C.P. of horizontal empennage (m),

M_H, moment of horizontal empennage with respect to C.G. of airplane (mkg),

ρ, angle of setting of horizontal empennage with respect to wing chord,

α_{mH_0}, angle of attack of wing at which $c_{mH} = 0$.

When same symbols are used for horizontal empennage as for wing, the former are denoted by the subscript H.

M_g, total moment of airplane (wing + empennage) with respect to C.G. (mkg),

α_A, angle of attack of moment balance,

c_{mg}, moment coefficient of whole airplane with respect to C.G., including wing area and chord.

III. Development of Formulas and Consideration of Stability

1. Wing Moment and Wing Moment Coefficient

The moment of the wing about its leading edge is given by the formula

$$M = c_m \, q \, F \, t \tag{1}$$

If this moment is referred to the airplane C.G., it then becomes

$$M_F = c_{mF} \, q \, F \, t$$

$$= \left(c_m + c_n \frac{r}{t} - c_t \frac{h}{t} \right) q \, F \, t \tag{2}$$

The C.G. is here considered as being forward of the leading edge of the wing (Fig. 1). Nose-heavy moments are considered positive and tail-heavy, negative. Accordingly, r is positive when the

C.G. is forward of the leading edge and negative when the C.G. is aft of the leading edge of the wing.

The term $c_t \frac{h}{t}$ in equation (2), which denotes the height of the C.G., is generally very small and has but a slight effect on the wing moment. Hence it is disregarded in our calculations. We thus obtain the simplified formula

$$M_F = \left(c_m + c_n \frac{r}{t}\right) q\ F\ t$$

or

$$c_{mF} = \frac{M_F}{q\ F\ t} = c_m + c_n \frac{r}{t} \qquad (3)$$

If the moment coefficient c_m is plotted against the lift coefficient c_a, the function $c_m = f(c_a)$ represents a straight line for almost all profiles in the normal range. Separation phenomena cause deviations which generally diminish with increasing Reynolds Number. If the moment coefficient for $c_a = 0$ is designated by c_{m_0} (Fig. 2), $c_m = f(c_a)$ can then be represented by the equation

$$c_m = c_{m_0} + \frac{d\ c_m}{d\ c_a} c_a \qquad (4)$$

The course of the function $c_m = f(c_a)$ is practically independent of the aspect ratio of the wing (Ergebnisse der Aerodynamischen Versuchsanstalt zu Göttingen, Report I, page 51), so that c_{m_0} is a constant quantity for all aspect ratios. Moreover, according to the hydrodynamic theory of the wing sections, $c_m = f(c_a)$ is a straight line with a 4 : 1 slope for

all profiles independently of the camber. The Göttingen wind-tunnel tests yield the same result. Hence $\frac{d\,c_m}{d\,c_a} = \frac{1}{4}$ is a constant quantity for all profiles. Equation (4) then becomes

$$c_m = c_{m_0} + 0.25\, c_a \qquad (4a)$$

If we put approximately $c_n = c_a$, then equation (3) (under consideration of equation (4a)) becomes

$$c_{mF} = c_{m_0} + c_a \left(0.25 + \frac{r}{t}\right) \qquad (5)$$

It is now desired to replace c_a by a function of α. If $c_a = f(\alpha)$ is plotted for different profiles but the same aspect ratio (Fig. 3), it is found:

1. That almost all curves are straight lines in the normal range up to c_a = about 1;

2. That all these curves are nearly parallel in the constant region.

In the constant region of the curves, $\frac{d\,c_a}{d\alpha}$ is therefore constant and has approximately the same value for all profiles. For the aspect ratio 5 the Göttingen profile measurements yield a mean value

$$\frac{d\,c_a}{d\,\alpha_s} = 0.0715 \qquad (6)$$

For the same c_a, different angles of attack α correspond to wings of different aspect ratios. Hence, $\frac{d\,c_a}{d\alpha}$ also varies with the aspect ratio, so that

$$\frac{d\,c_a}{d\,\alpha} = \frac{d\,c_a}{d\alpha'}\,\frac{d\alpha'}{d\alpha} \qquad (7)$$

which, after the differentiation $\frac{d\alpha'}{d\alpha}$, becomes

$$\frac{d\,c_a}{d\,\alpha} = \frac{d\,c_a}{d\alpha'} \frac{1}{1 - 57.3\,\psi \frac{d\,c_a}{d\,\alpha'}} \tag{8}$$

where

$$\psi = \frac{1}{\pi}\left(\frac{F'}{b'^2} - \frac{F}{b^2}\right)$$

If, in agreement with the Göttingen measurements, we put

$$\frac{F}{b^2} = \frac{1}{5}$$

and

$$\frac{d\,c_a}{d\alpha'} = \frac{d\,c_a}{d\,\alpha_s} = 0.0715$$

Equation (8) then becomes

$$\frac{d\,c_a}{d\,\alpha_0} = \frac{0.0548}{0.567 + \frac{F}{b^2}} \tag{9}$$

Figure 4 shows $\frac{d\,c_a}{d\,\alpha_0}$ plotted against the aspect ratio Λ. The curve $\frac{d\,c_a}{d\,\alpha} = f(\Lambda)$ shows that $\frac{d\,c_a}{d\,\alpha}$ undergoes very great changes at small aspect ratios, but that the changes are relatively unimportant at large aspect ratios (above 10).

We now measure the angle of attack from zero lift up and use the theoretical angle of attack

$$\alpha_{th} = \alpha - \alpha_0 \tag{10}$$

*Horst Müller, on the basis of American measurements (Zeitschrift fur Flugtechnik und Motorluftschiffahrt, 1929, p. 50), obtains

$$\frac{d\,c_a}{d\,\alpha_0} = \frac{0.0548}{0.562 + \frac{F}{b^2}}$$

where α_0 is the angle of attack corresponding to $c_a = 0$, and α corresponds to the geometrical angle of attack of the wing. The lift coefficient then becomes

$$c_a = \alpha_{th} \frac{d\, c_a}{d\, \alpha} \tag{11}$$

Substituting equations (10) and (11) in equation (5), we then obtain

$$c_{mF} = c_{m_0} + (\alpha - \alpha_0) \frac{d\, c_a}{d\alpha} \left(0.25 + \frac{r}{t}\right) \tag{12}$$

for the moment coefficient of the wing with respect to the airplane C.G. The decisive slope of the moment line for the degree of stability then becomes

$$\frac{d\, c_{mF}}{d\, \alpha} = \frac{d\, c_a}{d\, \alpha} \left(0.25 + \frac{r}{t}\right) \tag{12a}$$

The accuracy of the approximate method is indicated by Figure 5, in which the wing-moment curve obtained by calculating one point at a time (continuous line) is compared with the curve obtained by means of the approximation formula (dot-and-dash line). These two methods give almost identical results within the range of normal flight. The discrepancy at larger angles of attack or larger c_a is unimportant, since the main requirement is sufficient accuracy for the moments to balance. In general, it is required that in normal flight, according to the structural viewpoints for $\left(\frac{c_a}{c_w}\right)_{max}$ or $\left(\frac{c_a^3}{c_w^2}\right)_{max}$, $\Sigma M = 0$, that is, the moments must balance. Since the corresponding lift coefficient normally lies between $c_a = 0.7$ and 1, the utility

of the formula is demonstrated, for the agreement of the approximate and accurate calculation methods is very satisfactory within this range.

2. Moment and Moment Coefficient of Horizontal Empennage

On the assumption of a constant mean pressure by the aerodynamic forces acting on the horizontal empennage, the moment of the latter, with respect to the C.G., is

$$M_H = - N_H \, l_H \tag{13}$$

where l_H is the distance between the C.G. of the airplane and the C.P. of the horizontal empennage (Fig. 6). The C.P. of the empennage may be assumed to lie at one-third of its chord aft of the leading edge. Now

$$N_H = c_{nH} \, q \, F_H$$

If we again put $c_{nH} = c_{aH}$ and employ the method explained in connection with the wing, we obtain for the moment of the horizontal empennage with respect to the C.G.

$$M_H = - \alpha_{H_{th}} \left(\frac{d \, c_a}{d \, \alpha} \right)_H q \, F_H \, l_H \tag{14}$$

We now construct the moment coefficient of the horizontal empennage with respect to the C.G. and the area and chord of the wing and define it as

$$c_{mH} = \frac{M_H}{q \, F \, t}$$

By the introduction of equation (14), the moment coefficient of the horizontal empennage becomes

$$c_{mH} = - \alpha_{H_{th}} \left(\frac{d\, c_a}{d\, \alpha}\right)_H \frac{F_H\, l_H}{F\, t} \qquad (15)$$

Now the theoretical angle of attack of the horizontal empennage $\alpha_{H_{th}}$ is still to be expressed through the angle of attack of the wing, the relation between the angle of attack of the wing and that of the empennage being determined by the angle of setting ρ of the empennage. From Figure 7 we obtain

$$\alpha_H = \alpha + \rho \qquad (16)$$

If, similarly to equation (10), we again designate by α_{H_0} the angle of attack of the empennage at which $c_{aH} = 0$, we then have

$$\alpha_{H_{th}} = \alpha + \rho - \alpha_{H_0} \qquad (17)$$

Introducing this value into equation (15), we obtain

$$c_{mH} = - (\alpha + \rho - \alpha_{H_0}) \left(\frac{d\, c_a}{d\, \alpha}\right) \frac{F_H\, l_H}{F\, t} \qquad (18)$$

as the moment coefficient of the empennage with respect to the airplane C.G., including the area, chord and angle of attack of the wing, and

$$\frac{d\, c_{mH}}{d\, \alpha} = - \left(\frac{d\, c_a}{d\, \alpha}\right)_H \frac{F_H\, l_H}{F\, t} \qquad (18a)$$

as the slope of the moment line. For the corresponding choice of the ratio $\frac{F_H\, l_H}{F\, t}$ we can obtain any desired slope at which the point $c_{mH} = 0$ is maintained for $\alpha_{H_{th}} = 0$.

3. Angle of Setting of Horizontal Empennage

As already mentioned in the introduction, an important advantage of the Ente, in comparison with an ordinary airplane, is the fact that, with the proper dimensions and arrangement of the horizontal empennage, stalling of the airplane in steady flight is rendered impossible. This must be accomplished by so adjusting the empennage with respect to the wing that the air flow along the empennage separates while the wing is still within the normal flight range. The decrease in the empennage moment then causes the airplane to nose over before the flow separates from the wing. The angle of setting of the empennage must not be so great, however, as to bring the empennage into the region of separation at favorably high angles of attack of the wing. In soaring flight, in passing through a zone of stronger up-current the empennage will enter the higher angle-of-attack region, or the region of separation, before the wing.

For our calculations we shall assume that the maximum lift of the empennage is reached at an angle of attack 2° below that of the wing. Hence the formula for the setting of the empennage, as compared with that of the wing, is

$$\alpha_{H\ max} - \rho = \alpha_{max} - 2^\circ$$

or

$$\rho = \alpha_{H\ max} - \alpha_{max} + 2^\circ \qquad (19)$$

4. Determination of the Calculation Factors

The determination of α_0 and c_{m_0} does not require the plotting of the curves $c_a = f(\alpha)$ and $c_m = f(c_a)$. In general, according to what has preceded

$$c_{m_0} = c_m - 0.25\, c_a \tag{20}$$

and

$$\alpha_0 = \alpha - c_a \frac{d\alpha}{d\, c_a} \tag{21}$$

In particular, corresponding to the Göttingen tests with models, we have, for an aspect ratio of 5,

$$\alpha_0 = \alpha - 14\, c_a \tag{21a}$$

Hence we simply take from the model tests a measured c_a value with the corresponding α or c_m and introduce these values into equations (20) and (21) or (21a). These equations apply, however, only within the range of the polars in which the profile drag may be regarded as constant. Actual conditions are generally most closely approximated by taking from the model tests a test point between $c_a = 0.5$ and 0.7. Under these conditions the deviation of the approximation formula from the actual value is practically zero within the mean flight range.

If, however, it is desired to determine the values c_{m_0} and α_0 from the curves $c_a = f(\alpha)$ and $c_m = f(c_a)$, the test points in the constant zone of these curves are joined by a straight line. Discrepancies are disregarded, especially for small c_a and c_m values. For large c_a values it is advisa-

ble to join the test points in the usual manner. It is then immediately apparent in which zone the curves are rectilinear, thus indicating the angle-of-attack range in which the formulas hold good. For profiles of medium camber, the function $c_a = f(\alpha)$ can always be assumed to be rectilinear up to $c_a = 1$, but for greater cambers it is often rectilinear above $c_a = 1$. Since the aspect ratio is known to have no effect on the function $c_m = f(c_a)$ and since the variation in the angle of attack through self-induction ($\Delta \alpha = 57.3 \psi c_a$) is likewise zero for $c_a = 0$, it is obviously indifferent for what aspect ratio the values α_0 and c_{m_0} are determined. The magnitude of the differential quotient $\frac{d c_a}{d \alpha}$ is given by equation (9) and can be taken from the curve $\frac{d c_a}{d \alpha} = f(\Lambda)$ (Fig. 4).

The calculation of the wing moment therefore requires four quantities, two of which, α_0 and c_{m_0}, must be determined from the model tests, while the other two, namely, the wing aspect ratio Λ and the C.G. location r/t, represent constructional data. For the empennage moment, α_{H_0} must be determined from the model tests. Likewise the empennage setting ρ must be determined from $\alpha_{H\,max}$ and α_{max}, while the remaining quantities (Λ_H, F_H l_H, and F t) are constructional data.

5. Determination of the Stability Condition

Equilibrium obtains, when the sum of all the moments is zero, that is, when

$$\Sigma M = M_F + M_H = 0$$

or, in nondimensional coefficients,

$$\Sigma c_m = c_{mF} + c_{mH} = 0 \qquad (22)$$

Stability is a property of the state of equilibrium. The stability of an airplane is therefore assured, when any disturbance of the normal flight attitude by outside forces produces a moment which restores the original state of equilibrium. An airplane is stable when an increasing angle of attack produces a restoring (positive) moment and when a decreasing angle of attack produces an upturning (negative) moment. Hence the stability condition is expressed by the formula

$$\frac{d\,M_g}{d\,\alpha} > 0$$

or

$$\frac{d\,c_{mg}}{d\,\alpha} > 0 \qquad (23)$$

In the Ente the wing exerts a positive stabilizing effect within the whole angle-of-attack range. The stabilizing effect of the horizontal empennage must therefore be negative throughout the whole angle-of-attack range. If the wing-moment coefficient c_{mF}, the moment coefficient of the horizontal empennage c_{mH} and the resulting total moment c_{mg} are plotted against the angle of attack, the principal moment diagrams possible for the Ente (if moment balance is possible anyway) are the ones shown in Figures 8-10.

Case 1.- Normal (Fig. 8), stability $\left(\frac{d\,c_{mg}}{d\alpha} > 0\right)$ and moment balance in the normal flight range $(\Sigma M = 0)$.

Case 2.- (Fig. 9), instability $\left(\frac{d\,c_{mg}}{d\alpha} < 0\right)$ and moment balance in the normal flight range.

Case 3.- (Figs. 10a-10c). The wing and empennage curves intersect the abscissa (α axis) at a common point. In this case all three states of equilibrium (stable, neutral and unstable) are possible. Any moment balance in the normal flight range is impossible, however, if the neutral state is disregarded, in which $\Sigma c_m = 0$ throughout the angle-of-attack range. In stable or unstable equilibrium the moment balance occurs at the common intersection point of the wing and empennage curves (i.e., at negative lift) and consequently lies far outside of the normal flight range.

From the consideration of Figures 8-10, we can draw the important conclusion that satisfactory stability within the normal flight range is possible for the Ente, only when the moment curve of the empennage intersects the abscissa (α axis) at a smaller angle of attack than the moment curve of the wing. If α_{mF_0} is the angle of attack of the wing at which $c_{mF} = 0$, and if α_{mH_0} is the angle of attack of the wing at which $c_{mH_0} = 0$, the equilibrium conditions may be expressed as follows:

$\alpha_{mF_0} > \alpha_{mH_0}$ yields stable equilibrium;

" = " " all kinds of equilibrium;

" < " " neutral equilibrium.

If $c_{mF} = 0$ is introduced into equation (12), we obtain

$$\alpha_{mF_0} = \alpha_0 - \frac{c_{m_0}}{\frac{d\, c_a}{d\alpha}\left(0.25 + \frac{r}{t}\right)} \tag{25}$$

If $c_{mH} = 0$ is introduced into equation (18), we obtain

$$\alpha_{mH_0} = \alpha_{H_0} - \rho \tag{26}$$

Moreover, the introduction of equations (25) and (26) into equation (24) makes it possible to express the fundamental condition for stable equilibrium within the normal angle-of-attack range of the Ente by

$$\alpha_0 - \frac{c_{m_0}}{\frac{d\, c_a}{d\alpha}\left(0.25 + \frac{r}{t}\right)} > \alpha_{H_0} - \rho \tag{27}$$

With the aid of this formula, it can be determined in any case whether stability and moment balance are possible within the usual angle-of-attack range under the given conditions. For a profile with fixed C.P., for which $c_{m_0} = 0$, equation (27) is simplified to

$$\alpha_0 > \alpha_{H_0} - \rho \tag{28}$$

The stability is increased by shifting the C.G. forward (equation 12a). The product of the area of the empennage times the lever arm of its moment $(F_H\ l_H)$ must then be likewise increased, if the wing chord and area, as also the angle of attack of the moment balance, are to remain the same (equation 18a). The effect of shifting the C.G. is proportional to the differ-

ence between α_{mF_0} and α_{mH_0}, as shown in Figures 11a and 11b. In both cases the location of the C.G. and the slope of the wing-moment lines $\left(\frac{d\, c_{mF_1}}{d\,\alpha}\right.$ and $\left.\frac{d\, c_{mF_2}}{d\,\alpha}\right)$ are the same. The angle of attack of the moment balance α_A remains constant. The difference lies in the fact that the difference between α_{mF_0} and α_{mH_0} is greater in Figure 11b than in Figure 11a. Despite equal increase in the slope of the wing-moment lines $\frac{d(c_{mF_2} - c_{mF_1})}{d\,\alpha}$, which is synonymous with equal advance of the C.G., the increase in the slope of the total-moment line $\frac{d(c_{mg_2} - c_{mg_1})}{d\,\alpha}$ is greater in Case 2. If unstable or neutral equilibrium prevails, but very little improvement can be effected even by the most extreme location of the C.G. Satisfactory stability within the normal flight range can never be attained by simply shifting the C.G. without the preliminary condition of a sufficiently great difference between α_{mF_0} and α_{mH_0}. Figure 12 shows that, with the same angle of attack of the moment balance and the same location of the C.G., the stability increases in proportion to the increase in the difference between α_{mF_0} and α_{mH_0}. In order to create the most favorable stability conditions, we must therefore strive to make α_{mF_0} as great as possible and α_{mH_0} as small as possible.

6. Effect of the Profile on the Stability

Equations (25) and (26) indicate that α_{mF_0} and α_{mH_0} generally depend on the characteristics of the profile. We shall

therefore consider the relations between the angle of attack, the lift and the moment, in order to obtain formulas for approximating the quantitative stability conditions.

In Figure 13 the c_{m_0} values taken from Göttingen model tests are plotted against α_0. The numbers next to the individual points are the Göttingen profile numbers. The function $c_{m_0} = f(\alpha_0)$ clearly indicates a certain regularity. Obviously, α_0 decreases as c_{m_0} increases.

$$c_{m_0} = - 0.015\ \alpha_0 \qquad (29)$$

can be written as the mean value according to Figure 13. Any simplification of the formula for the moment coefficient of the wing with the aid of equation (29) is not advisable, because the accuracy of said formula would thus be considerably diminished. On the other hand, both the preceding and the subsequent formulas can be used to advantage elsewhere, where it is more a question of estimating variations.

Figure 14 shows the relation between $c_{a\ max}$ and α_0. Usually the angle of attack for zero lift α_0 is inversely proportional to the maximum lift $c_{a\ max}$. Approximately,

$$c_{a\ max} = 0.075 \times (10^{\circ} - \alpha_0) \qquad (30)$$

Figure 15 shows that α_{max} and α_0 bear a relation similar to that between $c_{a\ max}$ and α_0 (Fig. 14). In general, α_{max} is inversely proportional to α_0. The actual relations would be difficult to determine, since other factors, such as the degree

of smoothness of the model, sometimes cause an earlier and sometimes a later separation of the flow. If the maximum angle of attack for zero lift is calculated ($\alpha_{th\ max} = f(\alpha_0)$, (Fig. 16), the linear relation between the angle of attack for maximum lift and the angle of attack for zero lift is more clearly shown, because the percentile discrepancies are then smaller, due to the greater range of the angle of attack. According to Figure 15, the mean α_{max} for an aspect ratio of 5 is

$$(\alpha_{max})_s = 13.5 - 0.26\ \alpha_0 \tag{31}$$

A change in the aspect ratio causes a change of

$$\Delta\alpha_{max} = 57.3\ \psi\ c_{a\ max}$$

in the value of α_{max}. In the above formula

$$\psi = \frac{1}{\pi}\left(\frac{F'}{b'^2} - \frac{F}{b^2}\right) = \frac{1}{\pi}\left(0.2 - \frac{1}{\Lambda}\right)$$

If we now introduce equation (30) for $c_{a\ max}$, we obtain

$$\Delta\alpha_{max} = 2.74^\circ - \frac{13.7^\circ}{\Lambda} + 1.37\ \alpha_0\left(\frac{1}{\Lambda} - 0.2\right) \tag{32}$$

Now,

$$\alpha_{max} = (\alpha_{max})_s - \Delta\alpha_{max}$$

$$= 10.76^\circ - \alpha_0\left(\frac{1.37}{\Lambda} - 0.014\right) + \frac{13.7^\circ}{\Lambda}.$$

The factor -0.014 is small in comparison with the other factors and is therefore disregarded. We thus obtain the simplified expression

$$\alpha_{max} = 10.8^\circ + \frac{1.37}{\Lambda}(10^\circ - \alpha_0) \tag{33}$$

With the aid of the ascertained relations between α_0 and c_{m_0}, as also between α_0 and α_{max}, we can obtain for α_{mF_0} and α_{mH_0} simple formulas which clearly show the profile effect.

On introducing the value of c_{m_0} according to equation (29) into equation (25), the latter becomes

$$\alpha_{mF_0} = \alpha_0 \left[1 + \frac{0.015}{\frac{d\, c_a}{d\, \alpha} \left(0.25 + \frac{r}{t} \right)} \right] \tag{34}$$

Aside from the angle of attack of zero lift, the only remaining variables are the C.G. location r/t and the aspect ratio in $\frac{d\, c_a}{d\, \alpha}$. A unit graph which, for a given aspect ratio, is not affected by any change in α_0, is obtained by plotting the ratio $\frac{\alpha_{mF_0}}{\alpha_0} = f\left(\Lambda, \frac{r}{t}\right)$ against r/t (Fig. 17). The function $\frac{\alpha_{mF_0}}{\alpha_0} = f\left(\Lambda, \frac{r}{t}\right)$ then represents a group of equilateral hyperbolas with the asymptotes $\frac{\alpha_{mF_0}}{\alpha_0} = 1$ and $\frac{r}{t} = -0.25$. Increasing the aspect ratio rapidly lessens its effect (Fig. 4). Further advance of the C.G. diminishes $\frac{\alpha_{mF_0}}{\alpha_0}$. Since α_0 (excepting symmetrical profiles and those with a fixed C.P.) always has a negative value, α_{mF_0} increases with increasing r/t. With increasing r/t, the shifting of the C.G. has less effect on α_{mF_0}.*

Equations (26) and (19), with the use of equation (33), yield

$$\alpha_{mH_0} = \alpha_{H_0} - 1.37 \left[\frac{1}{\Lambda_H} (10^\circ - \alpha_{H_0}) - \frac{1}{\Lambda} (10^\circ - \alpha_0) \right] + 2^\circ \tag{35}$$

The function $\alpha_{mH_0} = f(\alpha_{H_0})$ is a straight line. The differen-

*In contrast herewith and for a constant aspect ratio, the slope of the wing moment line increases proportionally with r/t (See equation (12a).

tial quotient $\frac{d\,\alpha_{mH_0}}{d\,\alpha_{H_0}} = 1 - \frac{1.37}{\Lambda_H}$ indicates that the slope of these lines depends only on Λ_H. Any change in α_0 or Λ produces a parallel displacement of the lines. The value of α_{mH_0} is diminished by increasing the value of α_0 or Λ under otherwise like conditions (like α_{H_0} and Λ_H). We shall now simplify equation (35) still further by putting $\frac{1.37}{\Lambda} \times (10^\circ - \alpha_0) = 1.5^\circ$ as the mean value for the term, which corresponds approximately to $\alpha_0 = 0^\circ$ (symmetrical wing profile!) and $\Lambda = 9$ or 10 and $\alpha_0 = -1^\circ$. The simplified formula then reads

$$\alpha_{mH_0} = \alpha_{H_0} - \frac{1.37}{\Lambda_H} \times (10^\circ - \alpha_{H_0}) + 3.5^\circ \qquad (35a)$$

The value of α_{mH_0}, as calculated by this formula, differs from the first value (equation 35) by the amount

$$\Delta = \frac{1.37}{\Lambda} \times (10^\circ - \alpha_0) - 1.5^\circ$$

Within the range $\Lambda = 8$ to 15 and $\alpha_0 = -5^\circ$ to 2°, the maximum discrepancy may amount to 1° or -0.8°. Since the preceding case involves only the estimation of variations, this discrepancy is justified with respect to the above assumptions. For the sake of greater clearness, the functions $\alpha_{mF_0} = f(\alpha_0)$ and $\alpha_{mH_0} = f(\alpha_{H_0})$ are both plotted in Figure 18. The continuous lines represent α_{mF_0} and the dash lines represent α_{mH_0}. $\Lambda = 10$ in the calculation of α_{mF_0}. The possible errors due to differences in aspect ratio are very slight within the limits of $\Lambda = 8$ to 15. If the quantities α_0 and r/t are given, α_{mF_0} can be read from Figure 18. α_{mH_0} is obtained in like manner,

when α_{H_0} and Λ_H are given. As Figure 18 shows,

$$\alpha_{mF_0} > \alpha_{mH_0}, \text{ when } \alpha_0 \geqslant \alpha_{H_0} \tag{36}$$

Stability can therefore be expected in the normal flight range only when $\alpha_0 > \alpha_{H_0}$, the difference being inversely proportional to the value of α_0. We have already mentioned that the stability conditions are favorable in proportion to the difference between α_{mF_0} and α_{mH_0}. If it is desired to obtain great stability, namely, the greatest possible difference between α_{mF_0} and α_{mH_0}, a wing profile with large α_0 and small α_{max} (in accord with Fig. 18) must be used, while the empennage must have a profile with small α_0 and large α_{max}, that is, $\alpha_{H_{th\ max}} \geqslant \alpha_{th\ max}$. In general, this may be stated as follows.

For satisfactory stability in normal flight the Ente requires a horizontal empennage for which the angle-of-attack range between zero and maximum lift is greater than for the wing.

According to Figure 14 and equation (30), the negative value of α_0 is proportional to the maximum lift, which in turn is proportional to the profile camber. Hence, if normal profiles are used, the empennage must have a greater camber than the wing. In this case the best profile for the wing appears to be one with a fixed C.P., with a greater camber for the empennage. If, however, a highly cambered profile is adopted for the wing, the empennage should have a slotted profile, for which the flow through the slot at large angles of attack delays the separation of the flow on the suction side and consequently yields

a considerably larger angle-of-attack and lift range than is possible with normal profiles.

While the choice of the profile is of only subordinate importance for the stability of normal airplanes, in the case of the Ente the correct profile choice is the decisive factor for satisfactory stability within the normal flight range.

IV. Stability Characteristics of Two Profiles

The suitability of two profiles as Ente profiles will be briefly discussed. In both cases the aspect ratio of the wing was $\Lambda = 10$, and of the empennage $\Lambda_H = 8$. The C.G. was located at 20% of the wing chord in front of the leading edge of the wing.

In the first example the Göttingen profile No. 652 was used for both wing and empennage (Fig. 19). As might be predicted from equations (27) and (36), stability was wanting. Nothing could be gained in this case, even by moving the C.G. forward, because the location required, even for neutral equilibrium, would produce excessive moments. If $\alpha_{mF_0} = \alpha_{mH_0}$, then equation (27), by solving according to r/t, gives the location of the C.G. necessary for neutral equilibrium.

$$\frac{r}{t} = \frac{c_{m_0}}{\frac{d\,c_a}{d\,\alpha}(\alpha_0 - \alpha_{mH_0})} - 0.25 \qquad (37)$$

For our special case $\frac{r}{t} = 3.45$, an impossible value. The condition for the validity of equation (37) is, however, that α_0

must be greater than α_{mH_0}. This is illustrated by the second example.

In Figure 20 profile No. 527 was used for the empennage. Advancing the C.G. produced a steeper slope of the wing-moment curve, whereby the point $\alpha = \alpha_0$; $c_{mF} = c_{m_0}$ remained independent of the location of the C.G. and of the aspect ratio of the wing. Now, if $\alpha_0 < \alpha_{mH_0}$, then, as shown by Figure 20, the instability is not lessened but only increased by advancing the C.G. Hence, when $\alpha_0 < \alpha_{mH_0}$, there is neither stable nor neutral equilibrium, but only unstable equilibrium. If $c_{m_0} = 0$, then α_{mF_0} has the same value for any location of the C.G. and for any aspect ratio. If it is desired to obtain practicable stability with the wing profile No. 652, the empennage must be slotted.

In Figure 21 the American N.A.C.A. profile M 12 with fixed C.P. was used for the wing, the Göttingen profile No. 527 serving as the basis for the empennage. There is here shown very good stability in the normal flight range for the above-mentioned C.G. location of $\frac{r}{t} = 0.2$. The stability can be still further increased by a further advance of the C.G. or by using a more highly cambered profile for the empennage. This example also shows the stability conditions with a floating elevator, it being assumed that the slope of the empennage curve is hereby diminished 25%. It is obvious that stability can be attained within the normal flight range even with a floating elevator. With a floating elevator the stability is greater, but the angle

of attack of the moment balance tends to diminish.

These examples confirm the predictions based on the previous statements regarding stability. They also show that the stability is inversely proportional to the wing camber with the maximum empennage camber. Since the symmetrical profile is excluded by its small lift coefficient, a good wing profile for the Ente, as already mentioned, is one with a fixed C.P. which has higher lift coefficients than a symmetrical profile. Unfortunately, the hitherto published results of tests with profiles having a fixed C.P. are inadequate, there being an especial lack of German data. Moreover, reference was made to the possibility of using slotted profiles for the empennage, with more highly cambered wings.

V. Summary

In the foregoing investigation the following approximation formulas were developed by disregarding the effect of the downwash from the horizontal empennage on the wing behind it and by also disregarding the effect of the height of the C.G., which is generally slight.

1. Moment coefficient of the wing

$$c_{mF} = c_{m_0} + (\alpha - \alpha_0) \frac{d\, c_a}{d\, \alpha} \left(0.25 + \frac{r}{t}\right) \qquad (12)$$

Slope of the moment line of the wing,

$$\frac{d\, c_{mF}}{d\, \alpha} = \frac{d\, c_a}{d\alpha} \left(0.25 + \frac{r}{t}\right) \qquad (12a)$$

2. Moment coefficient of the horizontal empennage with respect to the airplane C.G., including the area, chord and angle of attack of the wing

$$c_{mH} = - (\alpha + \rho - \alpha_{H_0}) \left(\frac{d\, c_a}{d\, \alpha}\right)_H \frac{F_H\, l_H}{F\, t} \qquad (18)$$

Slope of the moment line of the empennage,

$$\frac{d\, c_{mH}}{d\, \alpha} = - \left(\frac{d\, c_a}{d\, \alpha}\right)_H \frac{F_H\, l_H}{F\, t} \qquad (18a)^*$$

The quantities c_{m_0} and α_0 are best determined by the formulas

$$c_{m_0} = c_m - 0.25\, c_a \qquad (20)$$

and, when $\Lambda = 5$ (Göttingen model tests),

$$\alpha_0 = \alpha - 14\, c_a \qquad (21a)$$

c_a, α and c_m are taken from a test point of the profile test between $c_a = 0.5$ and 0.7.

For the angle of setting of the empennage the requirement was made that the maximum lift of the empennage must be reached at an angle of attack 2° below that of the wing. For the angle of setting of the empennage we then have the condition

$$\rho = \alpha_{H_{max}} - \alpha_{max} + 2^\circ \qquad (19)$$

The stability conditions of the Ente type were investigated with the aid of the derived formulas. It was found that the static longitudinal stability of the Ente depends largely on the profile used. The fundamental condition for attaining static

*The formulas for the moment coefficient of the wing and of the empennage can also be applied to a tail-steered airplane. In the case of the empennage the downwash of the wing must also be taken into consideration.

stability in the normal flight range is the fact that the moment curve of the empennage for small angles of attack must pass through zero as the moment curve of the wing. This fact can be expressed as follows. If moment balance is to exist for the Ente within the normal flight range and if stability is to prevail within the whole angle-of-attack range, the angle-of-attack range between zero and maximum lift must be greater for the empennage than for the wing. This fundamental stability condition for the Ente is expressed by the formula

$$\alpha_{mF_0} > \alpha_{mH_0} \tag{24}$$

or

$$\alpha_0 = \frac{c_{m_0}}{\frac{d\,c_a}{d\,\alpha}\left(0.25 + \frac{r}{t}\right)} > \alpha_{H_0} - \rho \tag{27}$$

With the aid of further approximations, it was demonstrated that

$$\alpha_{mF_0} > \alpha_{mH_0}, \quad \text{only when} \quad \alpha_0 \gg \alpha_{H_0} \tag{36}$$

The attainable stability for a given location of the C.G. is proportional to the difference between α_{mF_0} and α_{mH_0} or α_0 and α_{H_0}. Likewise, the effect of shifting the C.G. is proportional to the difference between α_{mF_0} and α_{mH_0} (Figs. 11a and 11b). This indicates that the empennage requires a more highly cambered profile than the wing. In this case the best way is to adopt a profile with a fixed C.P. for the wing and a more highly cambered profile for the empennage. If, however, a more highly cambered profile is adopted for the wing, a slotted

profile must then be used for the empennage. In this way stability and moment balance within the normal flight range can be attained with the elevator either locked or floating.

In conclusion a few profiles of medium thickness and different cambers were investigated with respect to their suitability for Ente airplanes.

Translation by Dwight M. Miner,
National Advisory Committee
for Aeronautics.

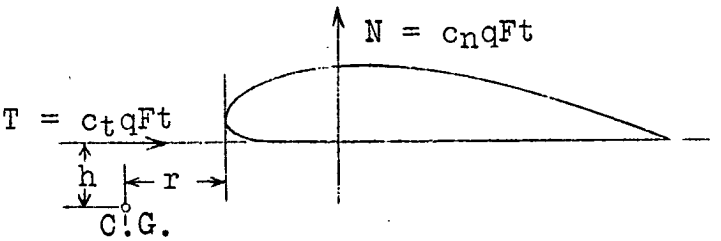

Fig.1 Determination of wing moment.

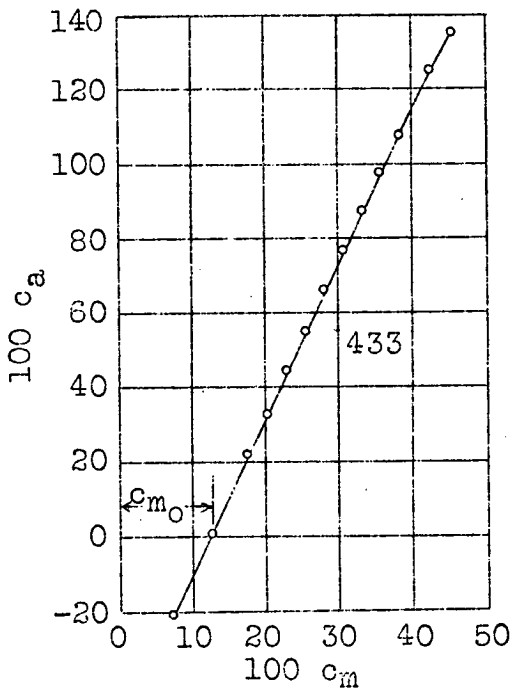

Fig.2
$c_m = f(c_a)$.

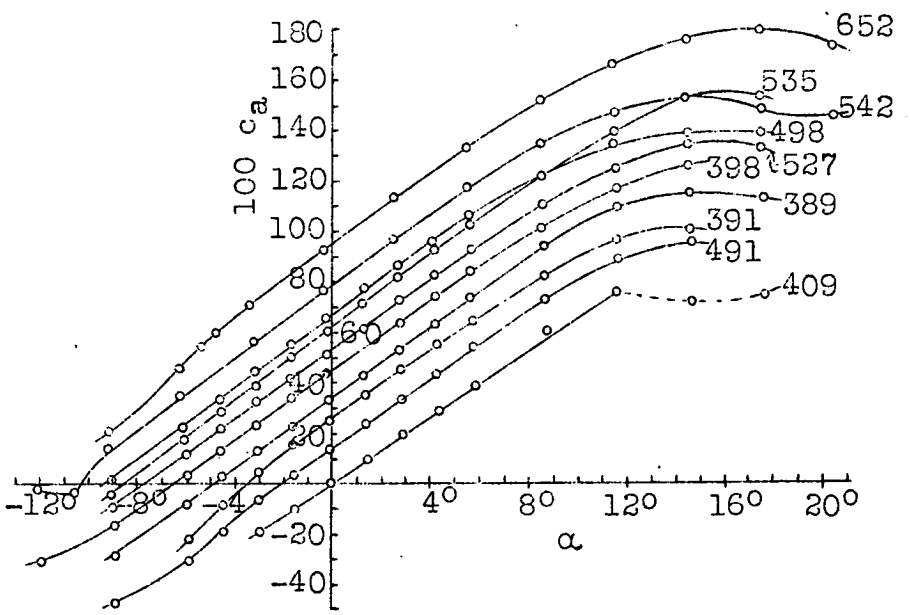

Fig.3 $c_a = f(\alpha)$ for various profiles ($\Lambda = 5$).

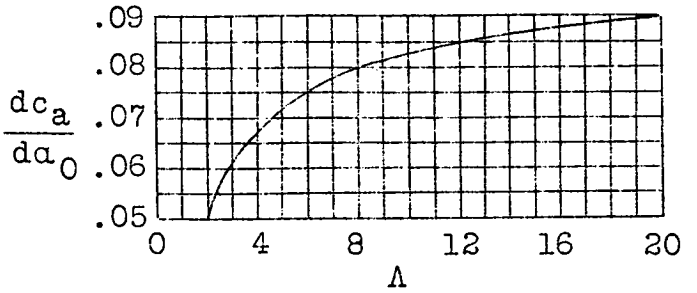

Fig.4 $dc_a/d\alpha_0$ plotted against aspect ratio Λ.

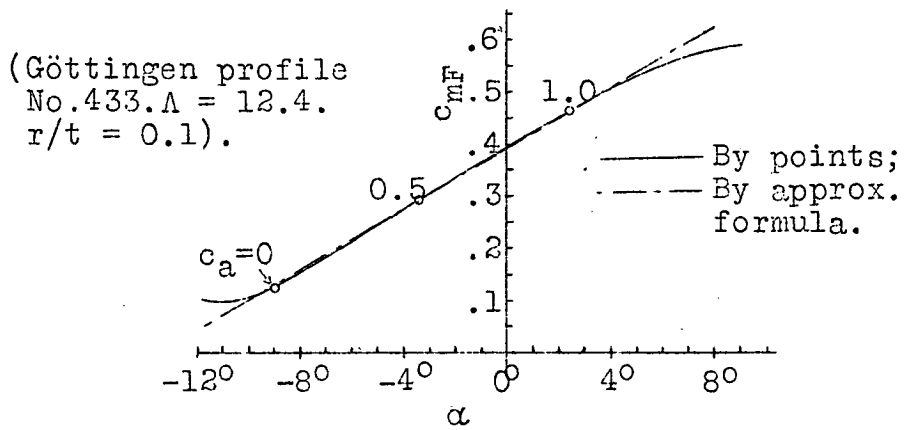

Fig.5 Comparison of wing-moment curves obtained by calculating one point at a time or by means of approximation formula 12.

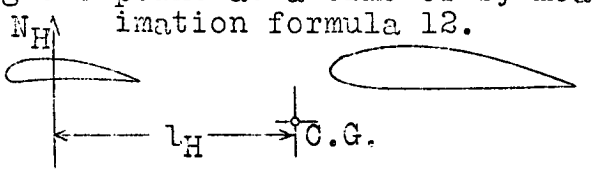

Fig.6 Determination of elevator moment.

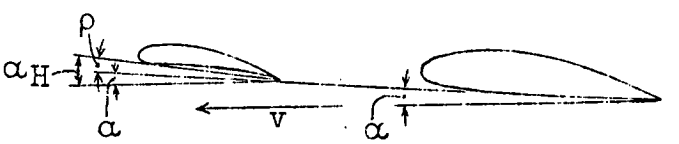

Fig.7 Relation between angle of attack of wing and of empennage.

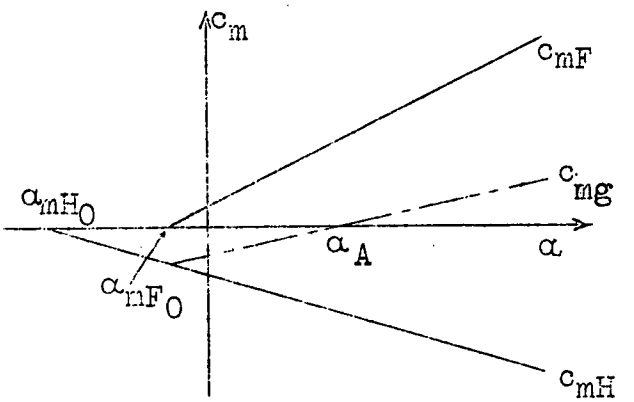

Fig.8 Normal case. Stability in normal flight range. ($\alpha_{mF_0} > \alpha_{mH_0}$. $dc_{mg}/d\alpha > 0$).

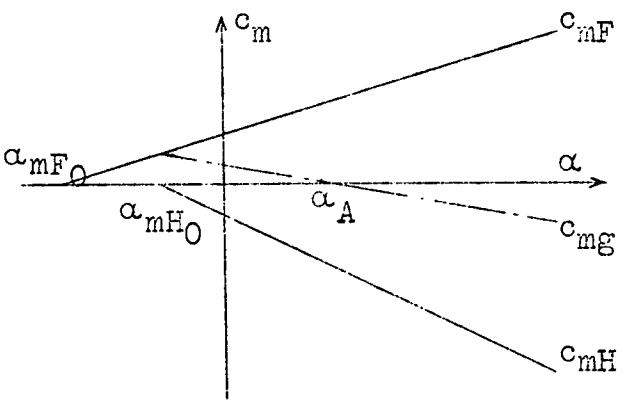

Fig.9 Instability in normal flight range. ($\alpha_{mF_0} < \alpha_{mH_0}$. $dc_{mg}/d\alpha < 0$)

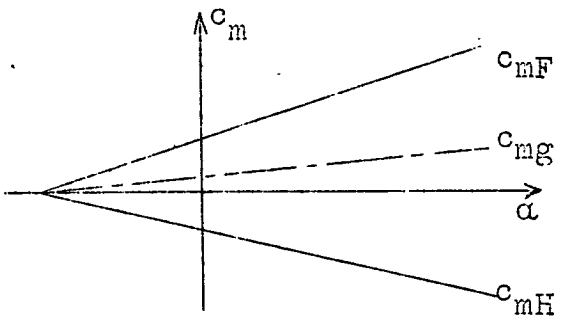

Fig.10a

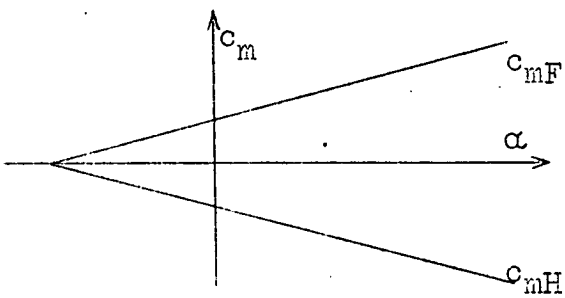

Fig.10b

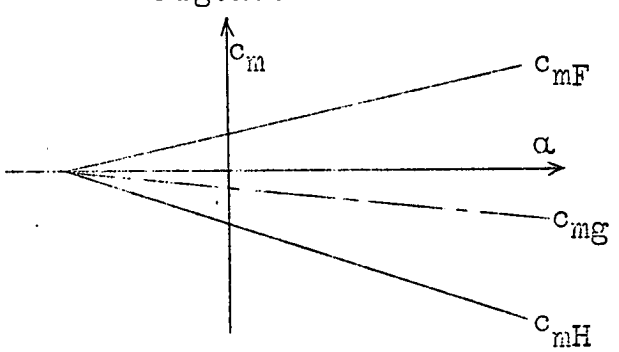

Fig.10c

Figs.10a,10b,10c. All states of equilibrium possible, but no moment balance in normal flight range. ($\alpha_{mF_0} = \alpha_{mH_0}$).

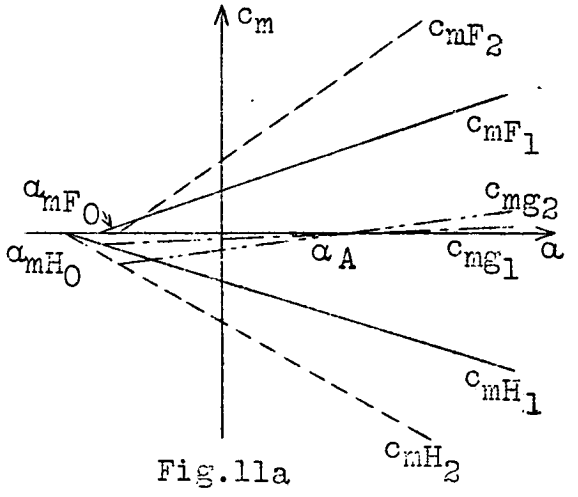

Fig.11a

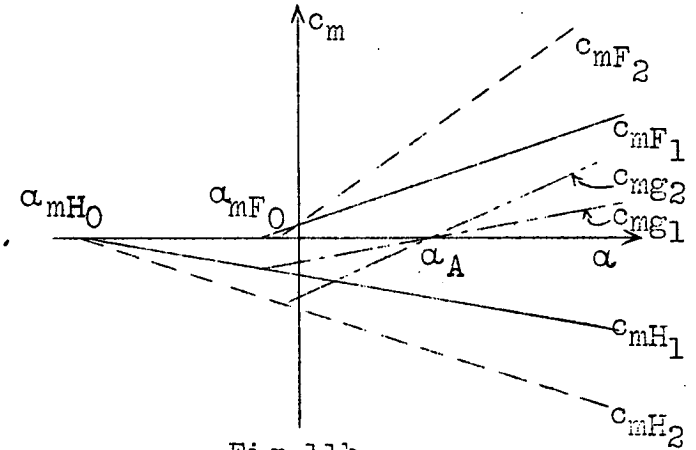

Fig.11b

Figs.11a,11b. For a given advance of C.G. with constant α_A, the increase in stability is proportional to the difference between α_{mF_0} and α_{mH_0}.
Subscript 1 = original C.G. location.
Subscript 2 = advanced C.G. location.
Case b $(\alpha_{mF_0} - \alpha_{mH_0}) >$ $(\alpha_{mF_0} - \alpha_{mH_0})$ Case a
Case b $\frac{d(c_{mg_2} - c_{mg_1})}{d\alpha} >$ $\frac{d(c_{mg_2} - c_{mg_1})}{d\alpha}$ Case a

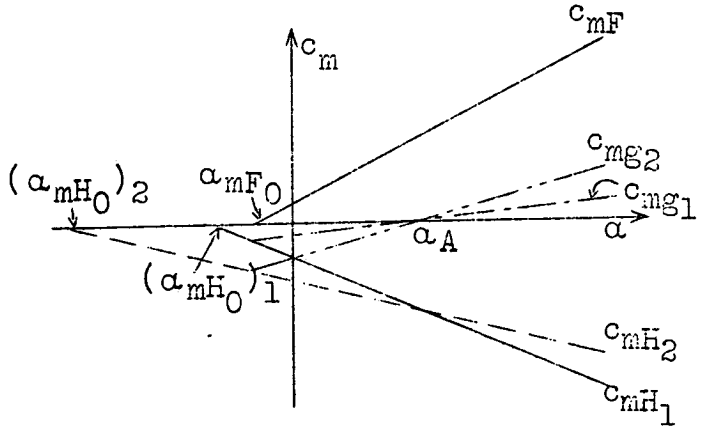

Fig.12 For a given C.G. location and α_A, the stability is proportional to the difference between α_{mF_0} and α_{mH_0}.
$\left((\alpha_{mF_0} - \alpha_{mH_0})_2 > (\alpha_{mF_0} - \alpha_{mH_0})_1;\ dc_{mg_2}/d\alpha > dc_{mg_1}/d\alpha\right)$.

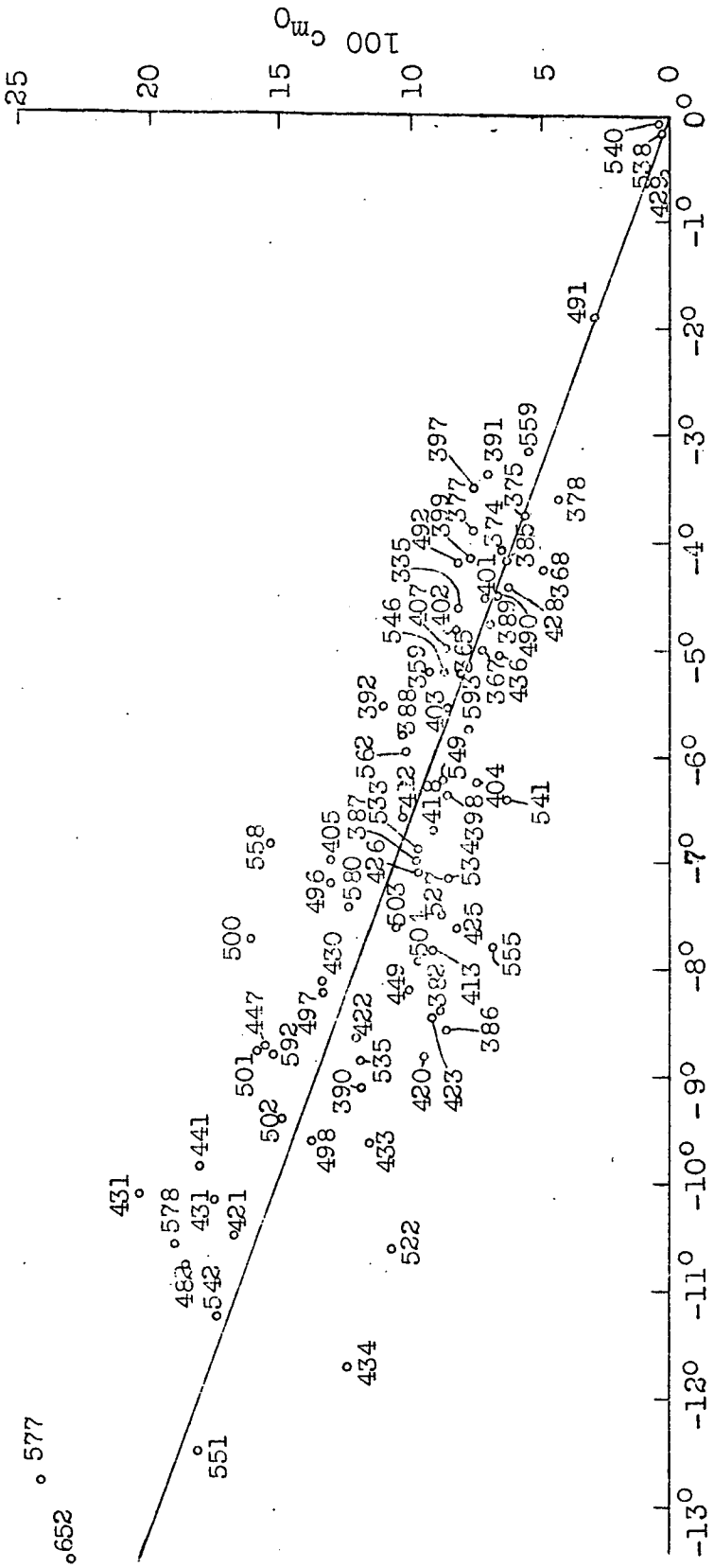

Fig.13 Relation between c_{m_0} and α_0.

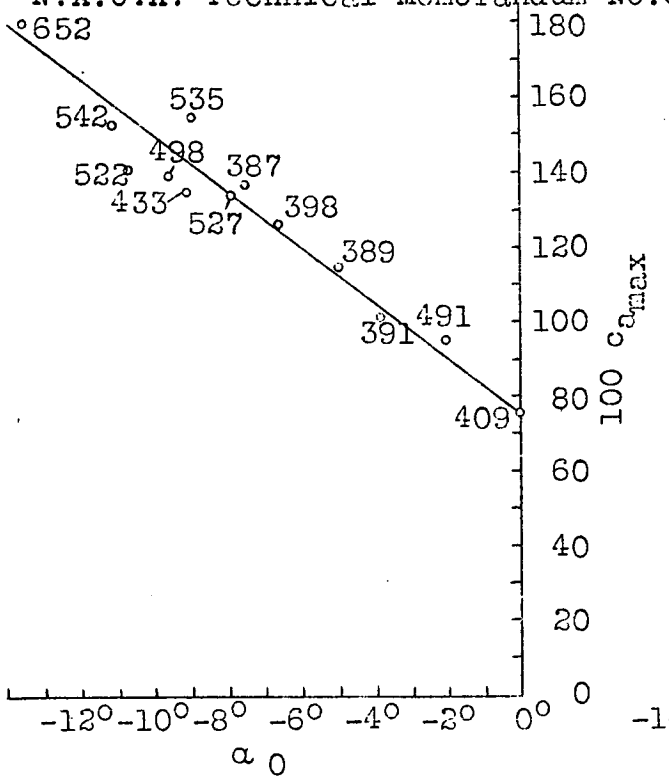

Fig.14 Relation between $c_{a_{max}}$ and α_0.

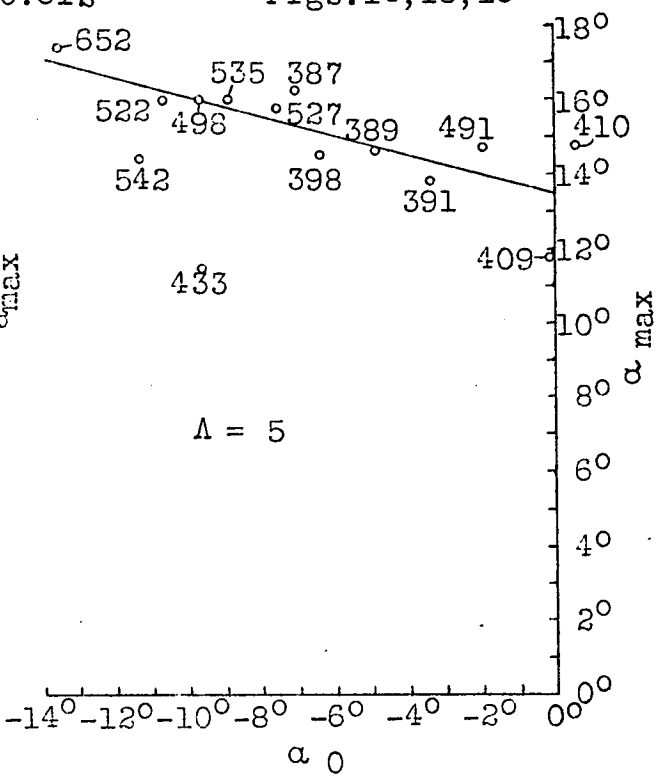

Fig.15 Relation between α_{max} and α_0.

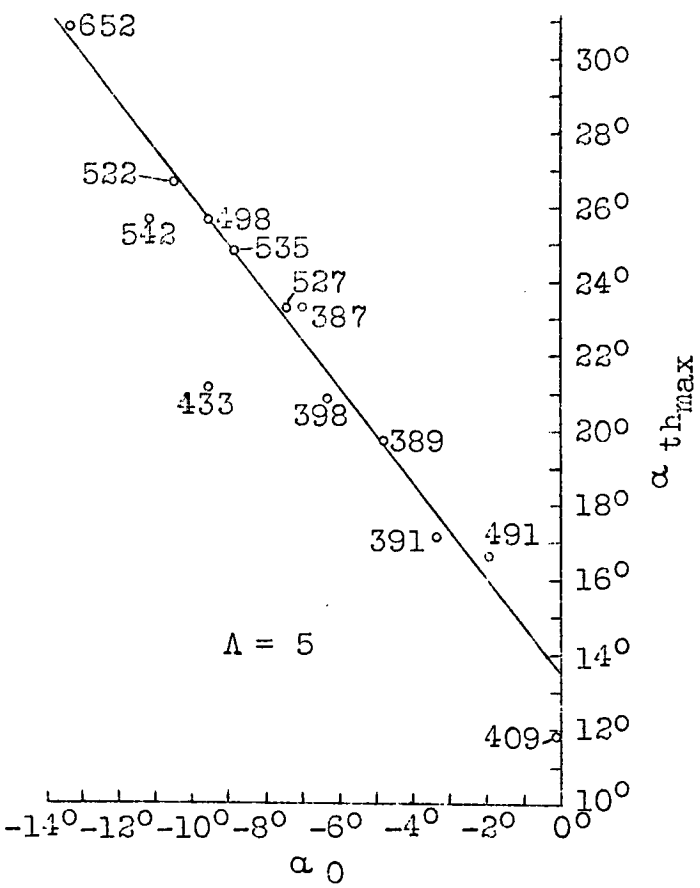

Fig.16 Relation between αth_{max} and α_0.

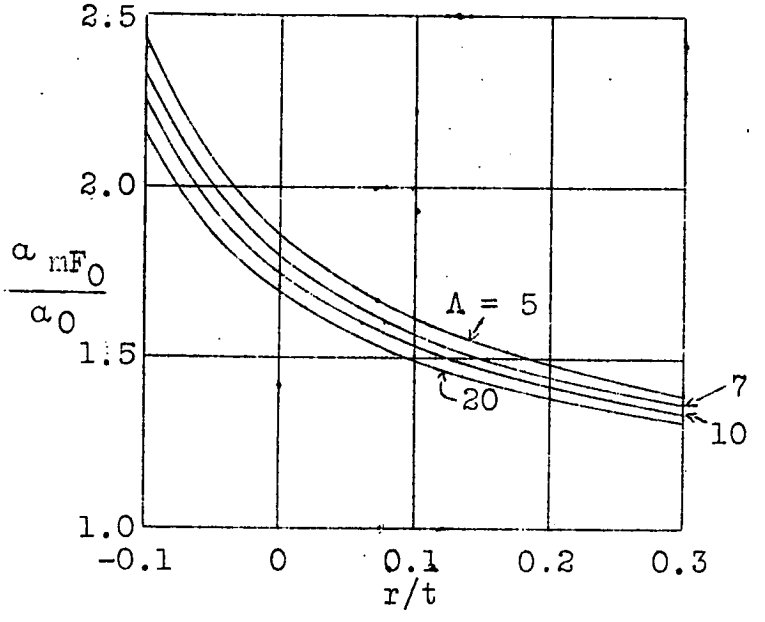

Fig.17 α_{mF_0}/α_0 plotted against C.G. location r/t.

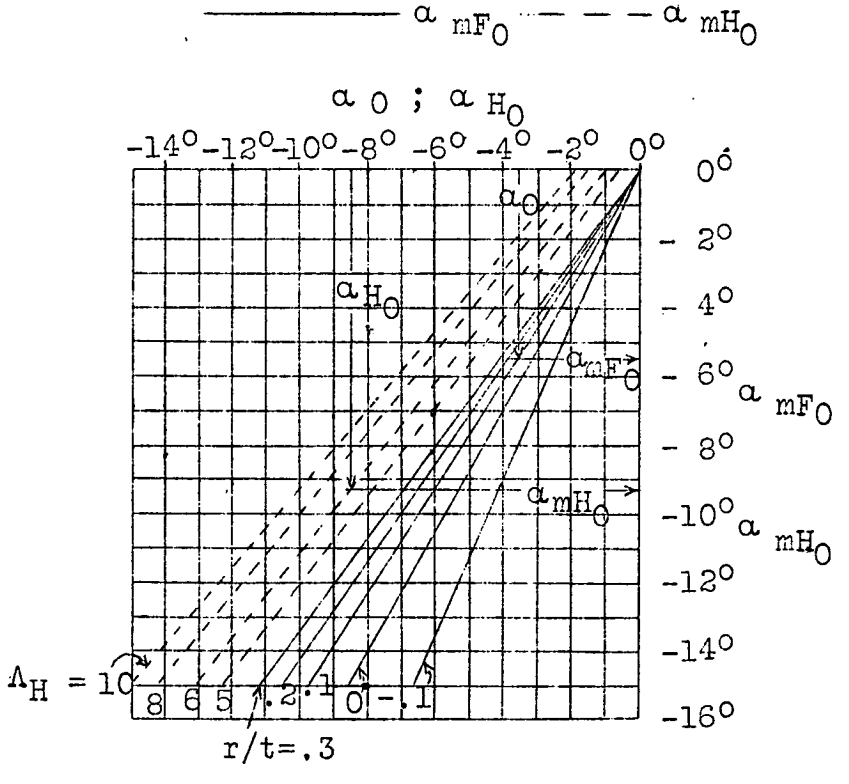

Fig.18 Determination of stability characteristics of profile combinations for wing and empennage. $\left(\alpha_{mF_0} = f(\alpha_0);\ \alpha_{mH_0} = f(\alpha_{H_0})\right)$.

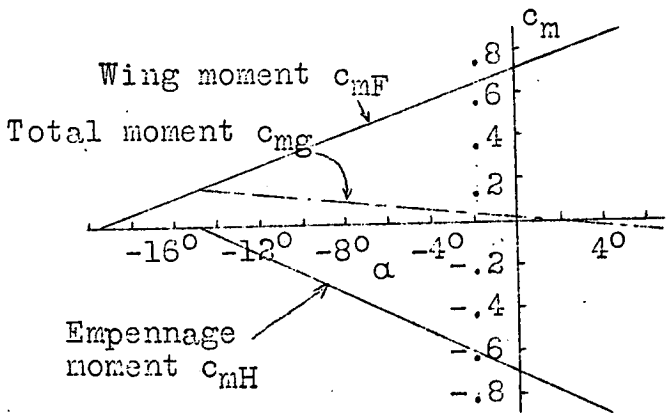

Fig.19 Moment diagram. Instability. Wing: Göttingen profile No.652. $\Lambda = 10$. Empennage: Göttingen profile No.652. $\Lambda_H = 8$. $r/t = 0.2$. $\rho = +1.3^\circ$

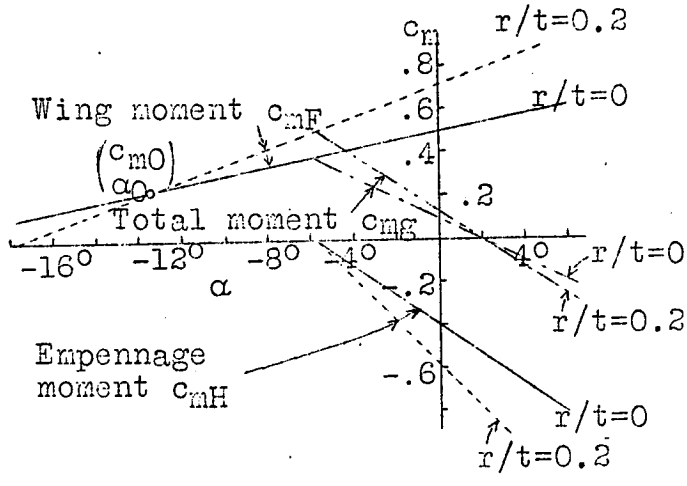

Fig.20 Moment diagram. Special case showing that instability is increased by shifting C.G. forward when $\alpha_{0} < \alpha_{mH_0}$.

Wing: Göttingen profile No.652. $\Lambda = 10$. Empennage: Göttingen profile No.527. $\Lambda_H = 8$. $r/t = 0.2$. $\rho = -0.5^\circ$.

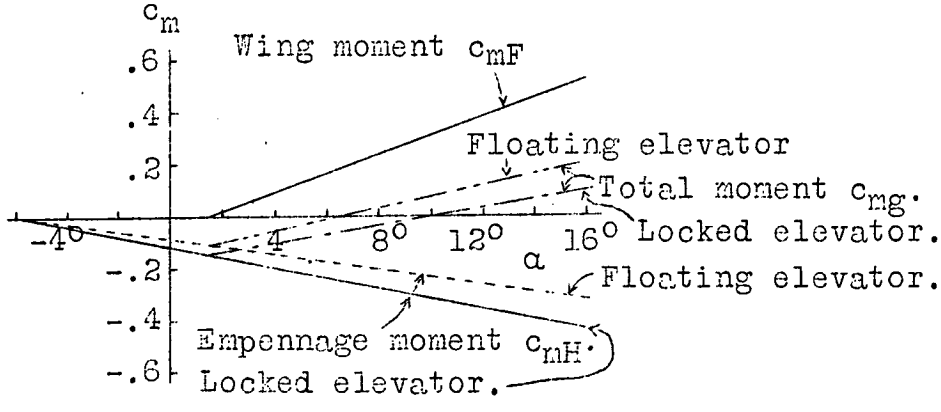

Fig.21 Normal moment diagram showing stability in normal flight range with locked elevator and with floating elevator. Wing: N.A.C.A. profile M12. $\Lambda = 10$. Empennage: Göttingen profile No.527. $\Lambda_H = 8$. $r/t = 0.2$. $\rho = -1.7^\circ$.